Supplementary Information

The Relative Insignificance of Polyamide Layer Selectivity for Seawater Electrolysis Applications

Environmental Science & Technology

Xuechen Zhou[1], Le Shi[1,2], Rachel Taylor[3], Chenghan Xie[1], Bin Bian[1], Cristian Picioreanu[4], and Bruce E. Logan[1,3*]

[1] Department of Civil and Environmental Engineering, The Pennsylvania State University, University Park, Pennsylvania 16802, USA.

[2] College of Environmental and Resource Sciences, Zhejiang University, Hangzhou 310058, P. R. China

[3] Department of Chemical Engineering, The Pennsylvania State University, University Park, Pennsylvania 16802, USA.

[4] Water Desalination and Reuse Center (WDRC), Biological and Environmental Science and Engineering Division (BESE), King Abdullah University of Science and Technology (KAUST), Thuwal 23955, Saudi Arabia

Number of Pages: 7

Number of Tables: 1

Number of Figures: 7

* Corresponding authors:

email: blogan@psu.edu; Tel. +1 (814) 8637908

S1. Electrode Preparation. Carbon cloth (2 × 2 cm^2) was first immersed into 4 M HCl solution and sonicated for 15 min. After that, it was cleaned using ethanol and DI water in sequence, sonicating for 15 minutes each time. The cleaned carbon cloth was then calcinated at 450 °C in the air overnight. To make each electrode, 40 mg 10% Pt/C powder, 267 µL 5 % Nafion solution, 133 µL isopropanol, and 33 µL DI were fully mixed by stirring for 3 hours. The mixed slurry was then applied to the treated carbon cloth using a brush. Finally, the electrodes were dried in air overnight before use.

Table S1. Parameters used in the numerical model.

Parameter	Description	Value	Unit
r_{p}	Pore radius of the pristine PA layer[1]	0.25	nm
$r_{\mathrm{Na^+}}$	Radius of sodium ions[a]	0.18	nm
$r_{\mathrm{K^+}}$	Radius of potassium ions[a]	0.13	nm
$r_{\mathrm{Cl^-}}$	Radius of chloride ions[a]	0.12	nm
$r_{\mathrm{ClO_4^-}}$	Radius of perchlorate ions[a]	0.14	nm
T	Absolute temperature	293.15	K
R	Gas constant	8.314	J K^{-1} mol^{-1}
F	Faraday constant	96485	C mol^{-1}
k_{B}	Boltzmann constant	1.38×10^{-23}	J K^{-1}
e	Elemental charge	1.6×10^{-19}	C
ε_0	Vacuum permittivity	8.85 x 10^{-12}	F m^{-1}
ε_{p}	Dielectric constant of the PA layer[2]	40	
ε_{b}	Dielectric constant of the bulk solution[2]	78	
$K_{\mathrm{d,i}}$	Diffusional hindrance factor for all ions, the same value[3]	0.01	
$D_{\mathrm{Na^+}}$	Sodium diffusion coefficient[4]	1.3x10^{-9}	m^2 s^{-1}
$D_{\mathrm{K^+}}$	Potassium diffusion coefficient[4]	2.0x10^{-9}	m^2 s^{-1}
$D_{\mathrm{Cl^-}}$	Chloride diffusion coefficient[4]	2.0x10^{-9}	m^2 s^{-1}
$D_{\mathrm{ClO_4^-}}$	Perchlorate diffusion coefficient[5]	1.8x10^{-9}	m^2 s^{-1}

D_{H^+}	Proton diffusion coefficient[4]	9.3x10^{-9}	m^2 s^{-1}
D_{OH^-}	Hydroxide diffusion coefficient[4]	5.3x10^{-9}	m^2 s^{-1}
ε	Effective porosity of the PA layer[6]	0.05	
$c_{m,c}$	Density of protonated amine groups[7]	30	mM
$c_{m,a}$	Density of residual carboxyl groups[7]	100	mM
$K_{a,a}$	Ionization constant for protonated amine groups[8]	10$^{-4.7}$	M
$K_{a,c}$	Ionization constant for carboxyl groups[9]	10$^{-5.2}$	M
K_w	Water dissociation constant	10^{-14}	M^2
ε_{sup}	Effective porosity of the support layer (skin layer)[10]	0.1	
ε_{elec}	Effective porosity of the platinum/carbon electrode[11]	0.1	
a_v	Specific surface area of the platinum/carbon electrode	1	mm^{-1}

[a] calculated based on Stokes–Einstein equation.

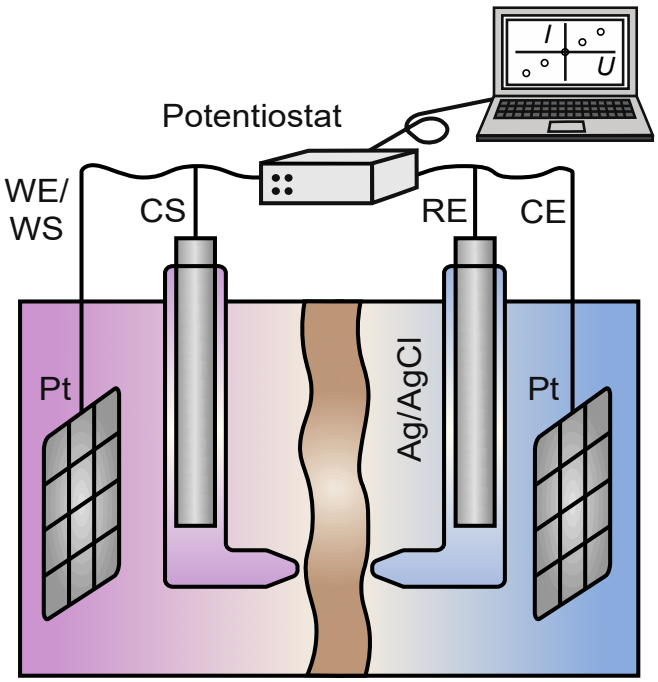

Figure S1. Schematic diagram showing the four-electrode system for the measurement of membrane resistance.

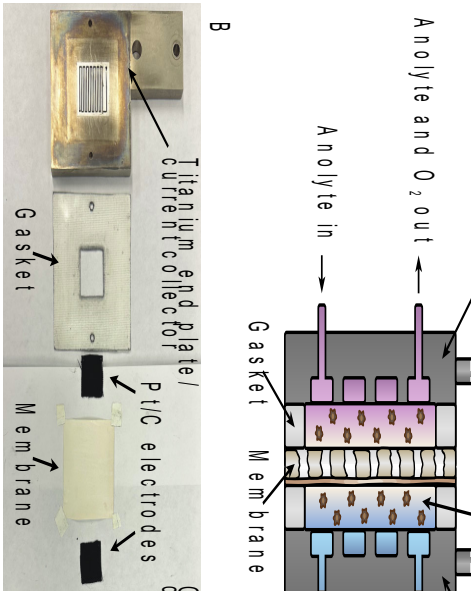

Figure S2. (A) Schematic diagram showing the design of zero-gap flow cell for seawater electrolysis. Pt/C electrodes were pressed on both sides of the separating membranes using end plates. Both the anolyte and catholyte were circulated at a flow rate of 15 mL min^{-1}. (B) Photograph of each component within the zero-gap flow cell.

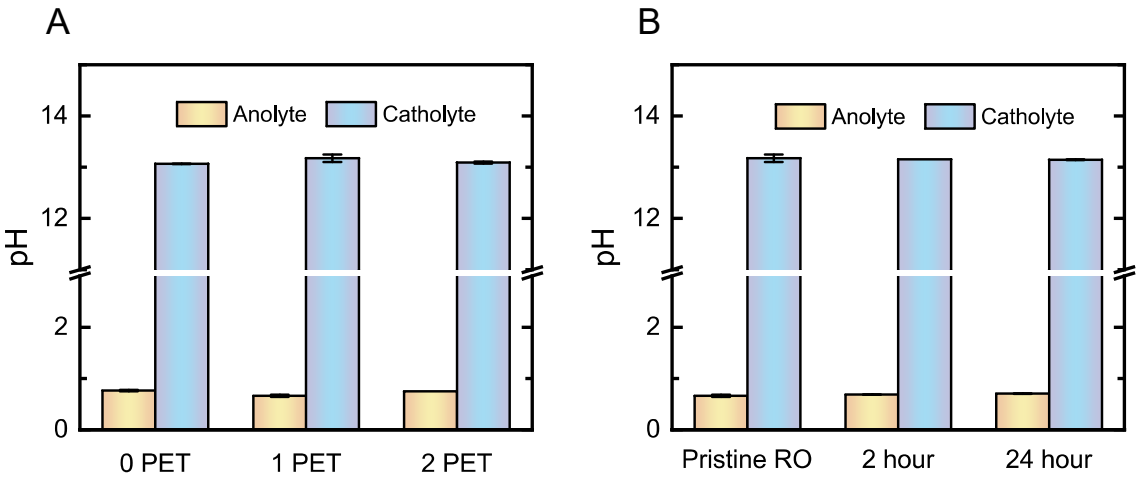

Figure S3. (A) pH of the electrolytes at the end of the operation of the electrolyzer assembled with the PA membranes with different number of PET layer. (B) pH of the electrolytes at the end of the operation of the electrolyzer assembled with PA membranes treated by NaClO by different durations.

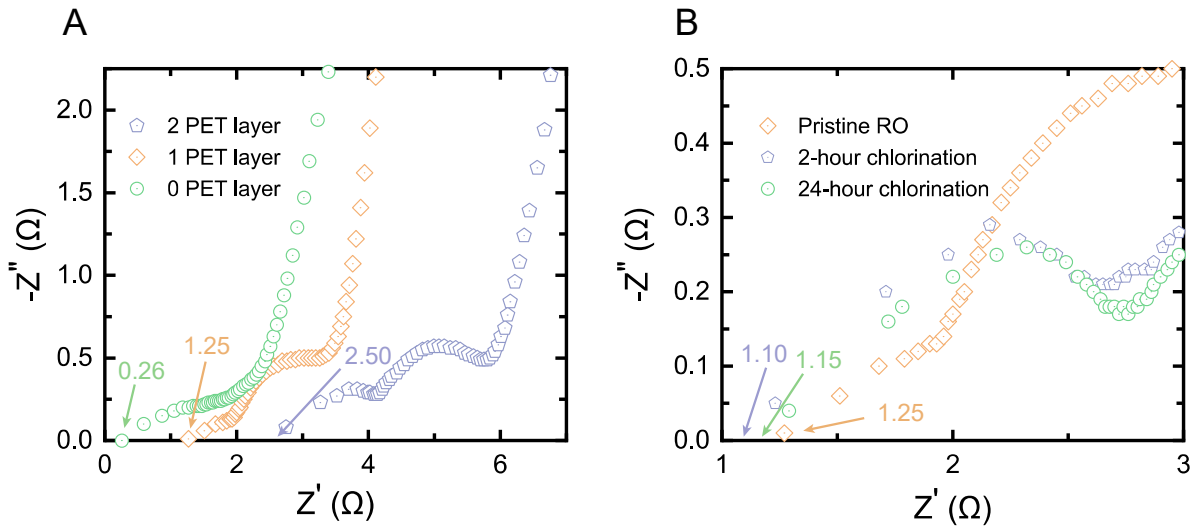

Figure S4. (A) Electrochemical impedance spectroscopy obtained at the end of the operation of the electrolyzer assembled with the PA membranes with different number of PET Layer. (B) Electrochemical impedance spectroscopy obtained at the end of the operation of the electrolyzer assembled with the PA membranes treated by NaClO by varied durations.

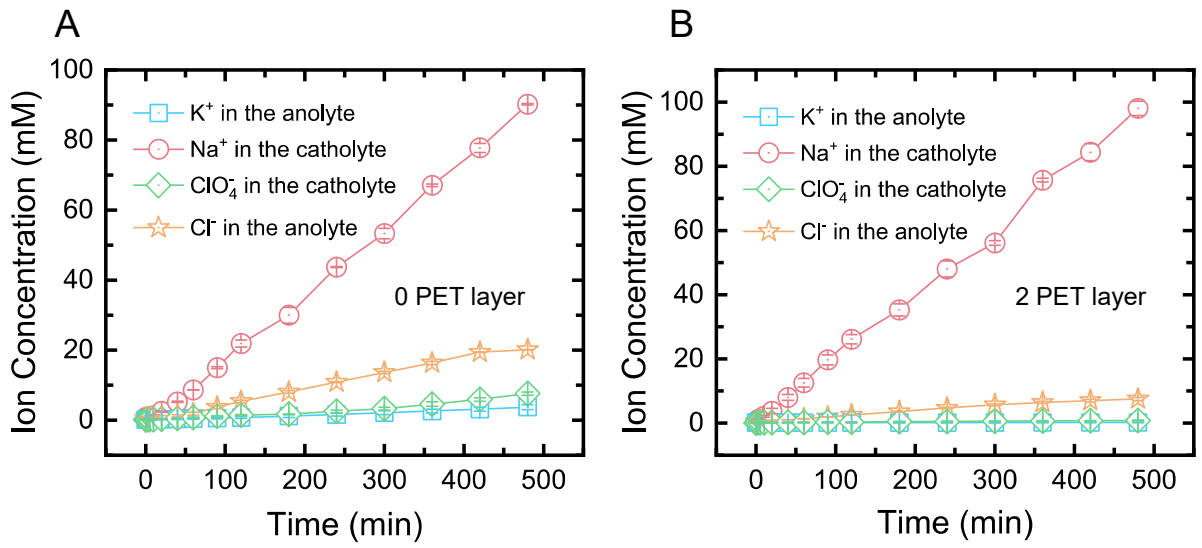

Figure S5. Ion permeation through the PA membranes with 0 and 2 PET layers within the electrolyzer.

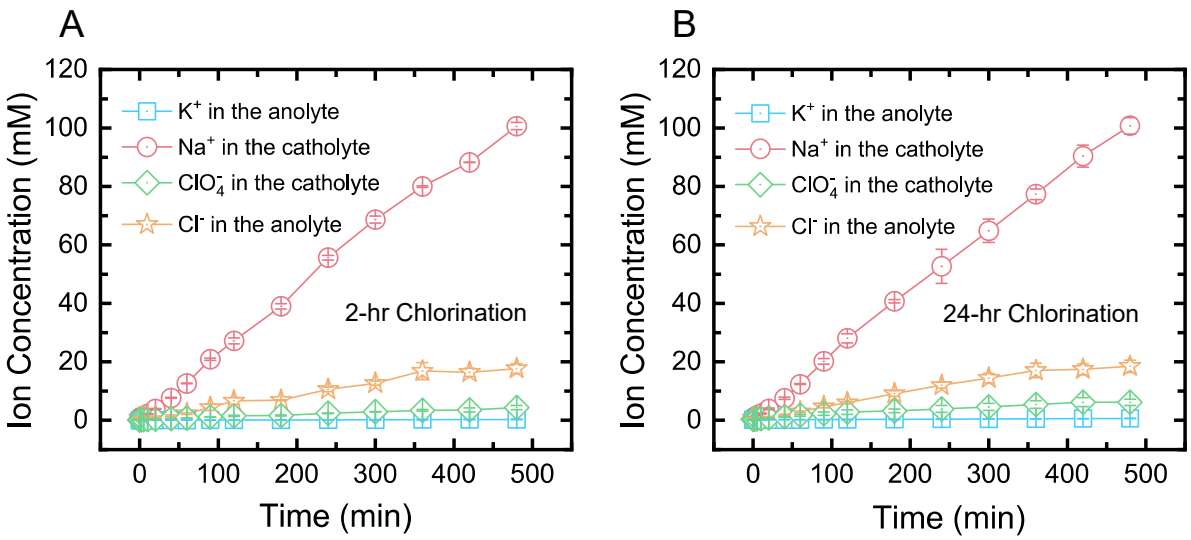

Figure S6. Ion permeation through the PA membranes treated with NaClO for 2 and 24 hrs within the electrolyzer.

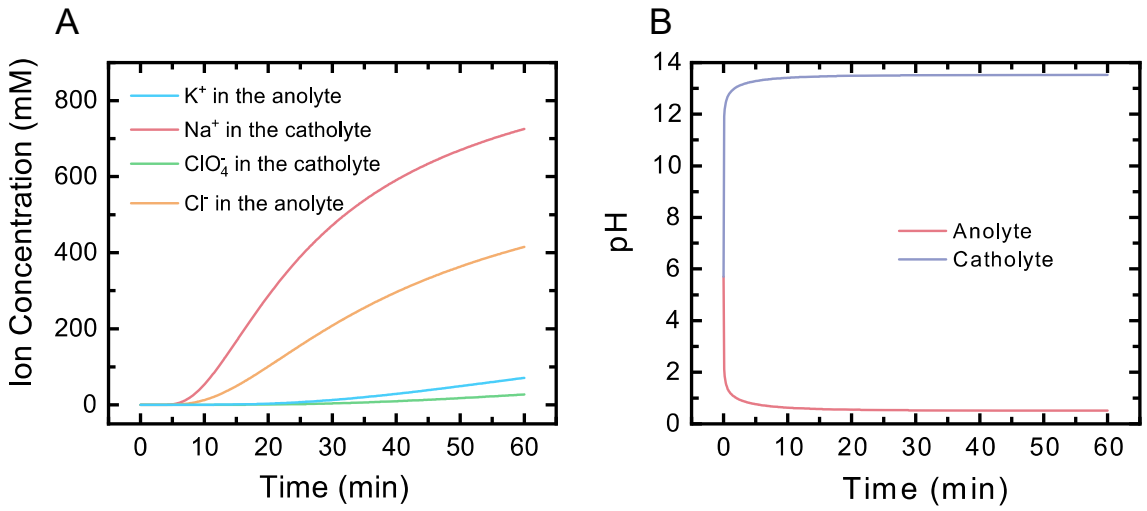

Figure S7. Calculated (A) ion permeation and (B) pH change of the electrolytes when using the pristine PA membrane for electrolysis.

REFERENCES

1. Davenport, D. M.; Ritt, C. L.; Verbeke, R.; Dickmann, M.; Egger, W.; Vankelecom, I. F. J.; Elimelech, M., Thin film composite membrane compaction in high-pressure reverse osmosis. *Journal of Membrane Science* **2020,** *610*.
2. Ritt, C. L.; Werber, J. R.; Wang, M. Y.; Yang, Z. Y.; Zhao, Y. M.; Kulik, H. J.; Elimelech, M., Ionization behavior of nanoporous polyamide membranes. *P Natl Acad Sci USA* **2020,** *117*, (48), 30191-30200.
3. Biesheuvel, P. M.; Zhang, L.; Gasquet, P.; Blankert, B.; Elimelech, M.; van der Meer, W. G. J., Ion Selectivity in Brackish Water Desalination by Reverse Osmosis: Theory, Measurements, and Implications. *Environmental Science & Technology Letters* **2020,** *7*, (1), 42-47.
4. Table of Diffusion Coefficient. *https://www.aqion.de/site/diffusion-coefficients*.
5. Banerjee, P.; Yashonath, S.; Bagchi, B., Rotation driven translational diffusion of polyatomic ions in water: A novel mechanism for breakdown of Stokes-Einstein relation. *Journal of Chemical Physics* **2017,** *146*, (16).
6. Wang, L.; Cao, T. C.; Dykstra, J. E.; Porada, S.; Biesheuvel, P. M.; Elimelech, M., Salt and Water Transport in Reverse Osmosis Membranes: Beyond the Solution-Diffusion Model. *Environmental Science & Technology* **2021,** *55*, (24), 16665-16675.
7. Stolov, M.; Freger, V., Membrane Charge Weakly Affects Ion Transport in Reverse Osmosis. *Environmental Science & Technology Letters* **2020**.
8. Kimani, E. M.; Pranic, M.; Porada, S.; Kemperman, A. J. B.; Ryzhkov, I. I.; van der Meer, W. G. J.; Biesheuvel, P. M., The influence of feedwater pH on membrane charge ionization and ion rejection by reverse osmosis: An experimental and theoretical study. *Journal of Membrane Science* **2022,** *660*.
9. Zhang, L.; Hamelers, H. V. M.; Biesheuvel, P. M., Modeling permeate pH in RO membranes by the extended Donnan steric model. *Journal of Membrane Science* **2020,** *613*.
10. Yakavalangi, M. E.; Rimaz, S.; Vatanpour, V., Effect of surface properties of polysulfone support on the performance of thin film composite polyamide reverse osmosis membranes. *Journal of Applied Polymer Science* **2017,** *134*, (6).
11. Yu, Z.; Carter, R. N.; Zhang, J., Measurements of Pore Size Distribution, Porosity, Effective Oxygen Diffusivity, and Tortuosity of PEM Fuel Cell Electrodes. *Fuel Cells* **2012,** *12*, (4), 557-565.